

This document is the Accepted Manuscript version of a Published Work that appeared in final form in ACS Sustainable Chemistry & Engineering, copyright © **2016 American Chemical Society** after peer review and technical editing by the publisher. To access the final edited and published work see <https://pubs.acs.org/doi/10.1021/acssuschemeng.6b00642>

DOI: <https://doi.org/10.1021/acssuschemeng.6b00642>

## **Willow lignin oxidation and depolymerization under low cost ionic liquid**

R. Prado<sup>a</sup>, X. Erdocia<sup>b</sup>, G. F. De Gregorio<sup>a</sup>, J. Labidi<sup>b</sup>, T. Welton<sup>a</sup>

a. Department of Chemistry, Imperial College London, Exhibition Road, SW7 2AZ, London, UK

b. Chemical and Environmental Engineering Department, University of the Basque Country, Plaza Europa 1, 20018, Donostia-San Sebastián, Spain

Corresponding author: [r.prado-garcia13@imperial.ac.uk](mailto:r.prado-garcia13@imperial.ac.uk)

Key words: Catalyst, heterogeneous, lignin, ionic liquids, oxidation.

### **Abstract**

Willow biomass was subjected to different pretreatment conditions with triethylammonium hydrogen sulfate as solvent and the produced lignin solutions were treated by oxidation either homogeneously using H<sub>2</sub>O<sub>2</sub> as oxidant, or by heterogeneous catalysis using TiO<sub>2</sub>. Lignin, residual lignin, oil and the recovered IL were characterized in order to determine the effects of each treatment. Lignin was successfully extracted and depolymerized by oxidation and characterized by ATR-IR, HPSEC and py-GCMS. The obtained oil was characterized by GCMS, it was composed mainly of acids derived from the sugar and lignin fractions, the TiO<sub>2</sub> catalyzed oils were richer in phenolic derived compounds than sugar fractions. The final ionic liquid was characterized in order to determine its suitability to be reutilized.

### **Introduction**

Recently, the quest for greener technologies that decrease our dependence on fossil fuels has become the principal target for many research groups. Efficient utilization of biomass is becoming increasingly important as it is the most abundant renewable material on earth, with a yearly global supply of approximately 200 billion metric tons<sup>1</sup>. Lignocellulose consists

mainly of plant cell wall material; it is a complex natural composite with three main biopolymers: cellulose (ca. 50%), hemicelluloses (ca. 25%) and lignin (ca. 25%)<sup>2</sup>. The structure and composition of lignocellulose varies greatly, depending on plant species, part of the plant and growth conditions<sup>1</sup>.

Lignin is a phenolic polymer synthesized via the oxidative coupling of three major C6-C3 phenylpropanoid units, namely, syringyl alcohol, guaiacyl alcohol and *p*-coumaryl alcohol, which form a complex and random three dimensional structure inside the cell wall which varies depending on the specie<sup>3</sup>. Lignin is the main by-product in chemical pulping processes, amounting to around 100 million tons per year, most of which is burned to generate energy which is reintegrated into the plant for its own energy supply. However, as lignin is the only renewable source of aromatic compounds, it can potentially be an important source of different products with a range of applications<sup>4</sup>. The diversity of functional groups present in lignin allows it to be used as a dispersant in cement and gypsum blends<sup>5</sup>, as an emulsifier or chelating agent for removing heavy metals from industrial effluent<sup>6</sup>, as a food additive, in batteries as a coating for graphite electrodes<sup>7</sup> and it has been added to composites as reinforcement<sup>8</sup>.

Willow is a commercially cultivated crop that has potential to be a dedicated biomass crop. Willow's leaves and bark are rich in compounds widely used in the pharmaceutical industry, well recognized throughout Europe for treating inflammatory conditions and pains of different origin. There are presently 24 willow varieties available that have been certified by the EU. There are 10 of commercial use today and approximately one-two varieties are developed annually<sup>9</sup>.

Room-temperature ionic liquids (ILs) are receiving a significant amount of interest owing to their characteristics as environmentally friendly solvents for a range of chemical processes both for catalyzed and uncatalyzed reactions, or as possible constituents in electrochemical

devices<sup>10,11</sup>. Thus the molecular design, synthesis and characterization of ILs have been the focus of many recent scientific investigations. Their unique properties, such as being liquid over a wide temperature range, having negligible vapor pressure and high thermal, chemical and electrochemical stability, allow a wide range of applications and make ILs good alternatives to environmentally harmful volatile organic solvents<sup>12</sup>. The properties of ILs vary enormously as a function of their molecular structure and considerable effort has been devoted to identifying and understanding those that have superior properties in any given application<sup>13,14</sup>.

It is well known that the structure of lignin is affected by the extraction processes, which cause chemical changes and fragmentation due to the chemical agents and conditions used<sup>15</sup>. This fact makes the study of how lignin is affected by each IL of paramount importance. For example, Tan *et al.* observed that after delignification of sugarcane waste using 1-ethyl-3-methylimidazolium alkylbenzenesulphonate ([C<sub>2</sub>C<sub>1</sub>im][ABS]), the obtained lignin had a lower average molecular weight (M<sub>w</sub>) than autocatalysis lignin. Both lignins were acetylated in order to allow comparison. Acetylated lignin from [C<sub>2</sub>C<sub>1</sub>im][ABS] had a lower M<sub>w</sub> (3690 g/mol) than acetylated autohydrolysis lignin (19300 g/mol), polydispersity was also lower for the [C<sub>2</sub>C<sub>1</sub>im][ABS] treated lignin (1.66 and 11.4 respectively)<sup>16</sup>. George *et al.* studied the effect of different ILs (1-ethyl-3-methylimidazolium n-hexylsulfate ([C<sub>2</sub>C<sub>1</sub>im][HxSO<sub>4</sub>]), 1-ethyl-3-methylimidazolium diethylphosphate ([C<sub>2</sub>C<sub>1</sub>im][Et<sub>2</sub>PO<sub>4</sub>]), 1-ethyl-3-methylimidazolium n-butylsulfate ([C<sub>2</sub>C<sub>1</sub>im][BuSO<sub>4</sub>]), 1-ethyl-3-methylimidazolium dimethylphosphate ([C<sub>2</sub>C<sub>1</sub>im][Me<sub>2</sub>PO<sub>4</sub>]), 1-ethyl-3-methylimidazolium lactate ([C<sub>2</sub>C<sub>1</sub>im][lac]), 1-ethyl-3-methylimidazolium chloride [C<sub>2</sub>C<sub>1</sub>im]Cl, 1-ethyl-3-methylimidazolium acetate ([C<sub>2</sub>C<sub>1</sub>im][Me<sub>2</sub>CO<sub>2</sub>]), 1-butyl-3-methylimidazolium chloride ([C<sub>4</sub>C<sub>1</sub>im]Cl), Cyphos 101, Cyphos 165 and 1-methyl-2-pyrrolidonium chloride ([C<sub>1</sub>pyr]Cl)) with lignin from different sources (organosolv, alkali (NaOH) and moderately sulfonated alkali lignin). It was observed

that the anion had more influence on the lignin structure than the cation. The effect of the anion in modifying lignin's molecular weight follows the order: sulfate>lactate>acetate>chloride>phosphate. It must be highlighted that the rate of modification of lignin by the action of IL also depends on its source, with organosolv lignin being more susceptible to structural changes than moderately sulfonated lignin and alkali lignin<sup>17,18</sup>.

Due to its complex structure, few investigations using lignin directly as a substrate have been conducted to study its reactivity. However, many studies have been carried out using lignin model compounds in order to elucidate the reaction mechanisms and the proper conditions to extend the reaction to lignin<sup>15</sup>. The depolymerization of lignin model compounds and lignin in ILs have been studied under both reductive and oxidative conditions. The reductive conditions were achieved by adding Lewis and Brønsted acids as a catalyst; however, these reactions were only briefly studied because of the low reactivity shown by lignin itself, despite the high yields obtained with lignin model compounds. Oxidation has been studied more extensively, in most cases coupling a metal catalyst such as Fe, Mn, Co, V, Pd, Mg and an oxidizing agent such as O<sub>2</sub>, H<sub>2</sub>O<sub>2</sub> or other peroxide acids with many different solvents and under different conditions<sup>15,19</sup>. The role of the ILs in this case was to be the reaction solvent and/or catalyst<sup>20</sup>. Three different species of willow (Resolution, Terranova and Endurance) were delignified by [Et<sub>3</sub>NH][HSO<sub>4</sub>] following the best conditions observed in previous experiments for Miscanthus<sup>21</sup>. In previous experiments, it was observed that [Et<sub>3</sub>NH][HSO<sub>4</sub>] showed lower overall yield than butylimidazolium hydrogensulphate [HC<sub>4</sub>im][HSO<sub>4</sub>] for lignin oxidation depolymerisation. In addition, the composition of the oil was different for both ILs. In this work we sought to improve the [Et<sub>3</sub>NH][HSO<sub>4</sub>] performance by adding a heterogeneous catalyst, as is less toxic than [HC<sub>4</sub>im][HSO<sub>4</sub>]. The obtained lignin was characterized and the

most suitable species was treated for different times and at different temperatures. The aim of the study was to establish which lignin was the best for oxidative depolymerization under different conditions using low cost ILs. The influence of heterogeneous and homogeneous conditions was studied by adding  $\text{TiO}_2$  and  $\text{H}_2\text{O}_2$  for the lignin obtained from each chosen willow species and pretreatment conditions.

## **Instruments**

All lignin samples were characterized by attenuated-total reflectance infrared spectroscopy (ATR-IR) by direct transmittance in a single-reflection ATR System (ATR top plate fixed to an optical beam condensing unit with ZnSe lens) with an MKII Golden Gate SPECAC instrument. Spectral data was acquired over 30 scans in the range of  $4000\text{-}700\text{ cm}^{-1}$  and  $4\text{ cm}^{-1}$  resolution.

The isolated lignin products were subjected to High Performance Size Exclusion Chromatography (HPSEC) to obtain lignin  $M_w$  and  $M_w$  distribution (MWD) using a JASCO instrument equipped with an interface (LC-NetII/ADC) and a refractive index detector (RI-2031Plus). Two PolarGel-M columns ( $300 \times 7.5\text{ mm}$ ) and PolarGel-M guard ( $50 \times 7.5\text{ mm}$ ) were employed. Dimethylformamide + 0.1% lithium bromide was used as the eluent. The flow rate was  $0.7\text{ mL min}^{-1}$  and the analyses were carried out at  $40\text{ }^\circ\text{C}$ . Molecular weight calibration was carried out using polystyrene standards (Sigma-Aldrich) ranging from 266 to  $70,000\text{ g mol}^{-1}$ .

GC-MS analysis was performed to identify and to quantify the monomers present in the oil. The oil was dissolved in ethyl acetate (HPLC grade) and was injected into an Agilent GC (7890A)-MS (5975C inert MSD with Triple-Axis Detector) equipped with a capillary column HP-5MS ((5%-Phenyl)-methylpolysiloxane,  $60\text{ m} \times 0.32\text{ mm}$ ). The temperature program

started at 50 °C raised to 120 °C at a rate of 10 °C min<sup>-1</sup>, held for 5 min, raised to 280 °C at a rate of 10 °C min<sup>-1</sup>, held for 8 min, raised to 300 °C at a rate of 10 °C min<sup>-1</sup> and finally held for 2 min. Helium was used as carrier gas. Calibration curves were established using commercially available compounds with purity >99% (Sigma-Aldrich) –phenol, o-cresol, m-cresol, p-cresol, guaiacol, catechol, 4-methylcatechol, syringol, acetovanillone, syringaldehyde, acetosyringone and 4-hydroxy-3-methoxyphenylacetone.

In order to determine the influence of the process on the nature of the IL and elucidate how the chemical structure of the IL is affected, ATR-IR spectral data was acquired over 30 scans in the range of 4000-700 cm<sup>-1</sup> and 4 cm<sup>-1</sup> resolution and NMR spectra were recorded at 30 °C on a Bruker Avance 600 MHz equipped with a z-gradient BBI probe. Typically, 40 mg of sample were dissolved in DMSO-d<sub>6</sub>. The spectral widths were 5,000 and 25,000 Hz for the <sup>1</sup>H and <sup>13</sup>C spectra, respectively.

High performance liquid chromatography (HPLC) analysis was performed on a Shimadzu Prominence HPLC with a photodiode array (PDA) detector. Detection of substrates was carried out at 280 nm using a Purospher STAR RP-18 end-capped column. A 20% Acetonitrile, 80% water isocratic method lasting 10 min was employed.

HSQC NMR spectra were recorded at 30 °C on a Bruker Avance 600 MHz equipped with a z-gradient BBI probe. Typically, 20 mg of sample was dissolved in 0.6 ml of DMSO-d<sub>6</sub>.

### **Synthesis of ionic liquid**

[Et<sub>3</sub>NH][HSO<sub>4</sub>] was synthesized by drop-wise addition of 5 M H<sub>2</sub>SO<sub>4</sub> to Et<sub>3</sub>N using an acid:base ratio of 1:1. An ice bath was used to maintain the temperature. The mixture was stirred for 24 h and dried under vacuum. The H<sub>2</sub>SO<sub>4</sub> was titrated prior to use in order to

determine its concentration as acid-base ratio has a large impact on pretreatment and the synthesis was performed in the way that deviation from 1:1 ratio was the minimum possible<sup>22</sup>.

### **Pretreatment**

Willow, water and [Et<sub>3</sub>NH][HSO<sub>4</sub>] were mixed in a 1:2:8 mass ratio. First the 3 different species of willow were pretreated at 120 °C for 22h<sup>21</sup>. The mixtures were subjected to different time and temperature conditions (150 °C 2 h, 120 °C 8 h and 120 °C 22 h) to establish the best conditions to obtain the most suitable lignin for oxidative depolymerization.

The resulting solution (black liquor) was filtered using Whatman 542 filter paper and washed with 3 volumes of ethanol. The ethanol of the black liquor was evaporated under vacuum at 55 °C.

### **Depolymerization**

In lignin depolymerization the performance of the heterogeneous and homogeneous conditions were compared. The black liquor was treated under oxidizing conditions with either 5% H<sub>2</sub>O<sub>2</sub> which acted as oxidant, or 1% TiO<sub>2</sub> as catalyst with 1% H<sub>2</sub>O<sub>2</sub>, which was required to initiate the reaction, for 1 h at 120 °C. The H<sub>2</sub>O<sub>2</sub> percentages were referred to an exact H<sub>2</sub>O<sub>2</sub> weight percent added from 30% H<sub>2</sub>O<sub>2</sub> commercially available solution.

The residual lignin was precipitated by the addition of 2 volumes of distilled water and then centrifuged at 4000 rpm for 15 min. The residual lignin was washed with distilled water and dried at 70 °C overnight.

The liquid phase was subjected to a liquid/liquid extraction process with MeTHF, in order to extract the small phenolic compounds. Extraction was repeated three times and the MeTHF was evaporated and resulting oil was characterized by GC-MS. The [Et<sub>3</sub>NH][HSO<sub>4</sub>] ionic liquid was recovered after centrifugation and dried by evaporation.

### **Results and discussion**



The main aim of this study was to establish which willow specie and pretreatment conditions provided the best lignin for being depolymerized under oxidative conditions, using either homogeneous or heterogeneous conditions. Three different willow species were treated by the same pre-treatment conditions. The lignin was characterized to establish which variety was the most suitable for its depolymerization and obtaining a higher quantity of phenolic monomers. Lignin was pretreated with the optimum conditions obtained before for *Miscanthus*<sup>21</sup>. The obtained lignin was characterized by HPSEC, py-GC-MS and HSQC NMR. Table 1 shows the yields obtained for the 3 species, the lignin yield was not significantly different according to the application of a one-way ANOVA test with significance level of 0.05, as the variance coefficient was found to be 0.04. The parameters that we took into account for determining which was the best specie to be depolymerized were: the  $M_w$  and the phenolic proportion of the lignin composition determined by py-GCMS (Figure 1). The  $M_w$  is important as higher  $M_w$  is normally associated with condensed structures that make lignin depolymerisation more difficult, as charge is delocalised along the aromatic structure of the lignin building strong internal linkages (Figure 2).

The heteronuclear single quantum coherence (HSQC)-NMR spectra of different lignin species are depicted in Figure 3 and the assigned structures are depicted in Figure 4, side chain region ( $\delta C/\delta H$  50–95/2.5–6.0 ppm) and the aromatic region ( $\delta C/\delta H$  95–160/5.5–8.0 ppm). 2D HSQC is a powerful tool for lignin structural characterization providing information of the structure of the inter-unit linkages present and was used to determine the differences in lignin structure depending on willow specie. The most common aromatic structures in lignins are those of phenylpropane origin, namely guaiacol alcohol, syringol alcohol and p-hydroxyphenyl alcohol. In Table 2 all the characteristic samples observed and their assignments are described. Table 3 shows the different proportion of the linkages observed for the different species, it was observed that Resolution showed of higher proportion of methoxyl groups and  $\beta$ -O-4 linkages

which are more suitable for being oxidised, on the other hand S/G ratio showed the same tendency observed by py-GCMS, where Resolution showed the lowest S/G ratio and Terranova the highest.

The Mw was determined by HPSEC, Table 1 shows the results obtained for the Mw for the different willow species. It was observed that lignin derived from Resolution has lower Mw compared to Terranova and Endurance; The MWD was also different for the three species; for Endurance a fragment was observed with a very high Mw and Resolution showed a narrower peak. The chromatograms were divided into 3 different regions depending on the nature of the compounds that were identified. The retention times are approximately related to the Mw of the fraction detected and its complexity. Products with a retention time between 3 to 11 min were identified as sugar fragmentation derived compounds, from 7 to 24.5 min, aromatic or phenolic fragmentation derived compounds were identified and finally long chain fatty acids fragments were identified post 24.5 min (Table 4). It was observed that Resolution willow had a higher proportion of phenolic derived compounds in its structure and Endurance and Terranova were richer in fatty acids and complex structures composed of more than one ring, such as 2-hydroxy-4-(phenylmethoxy)-benzaldehyde and condensed structures such as 1-phenanthrenecarboxylic acid. Overall it was decided to apply the consecutive depolymerization treatment for Resolution, as it had lower Mw and also a higher proportion of phenolic small fractions that can be easily extracted, or more easily broken down.

Different pre-treatment conditions were tested and the obtained yields relating to lignin are detailed in Table 5. The ANOVA statistics test was applied to the obtained yields to determine whether the pre-treatment conditions had any influence on depolymerization of lignin with a significance level of 0.05. The variance coefficient for biomass solubility was 0.01, implying

that yield was not significantly affected. The lignin recovery variance coefficient was 0.05, so lignin extraction was also not affected by pre-treatment conditions.

Results from the pretreatment yields did not indicate that lignin itself was affected. The obtained lignins were characterized by HPSEC, ATR-IR spectroscopy and py-GCMS. It was observed that the proportion of char was higher with lower reaction times and higher temperatures. Furthermore, the S/G ratio determined by py-GCMS was not significantly affected as the variance coefficient was 0.04.

Both lignin and residual lignin of all the different treatments were characterized by HPSEC, ART-IR spectroscopy and py-GCMS.

### **Oxidative depolymerization**

The three black liquors were subjected to oxidation. All the lignin samples were degraded under oxidizing conditions. Once again, the ANOVA statistics test with a significance level of 0.05 was applied to the lignin degradation yields and the oil extraction yields (Table 6). Lignin degradation was not significantly affected by pre-treatment conditions using  $\text{H}_2\text{O}_2$  under homogeneous conditions, as the obtained covariance coefficient was 0.05, but using  $\text{TiO}_2/\text{H}_2\text{O}_2$  the covariance coefficient was 2, implying that pre-treatment conditions affected the degradation of lignin. It was also observed that the highest degradation was obtained for Lig 2. On the contrary, comparing oil yields, for both conditions there was no significant difference in oil yield obtained, using  $\text{H}_2\text{O}_2$  the covariance coefficient was 0.04, but with  $\text{TiO}_2/\text{H}_2\text{O}_2$  the covariance coefficient was 0.07, and the best oil yield was obtained for Lig 2. To summarize, pre-treatment conditions affected the activity of heterogeneous catalysis with  $\text{TiO}_2$  and the best results were obtained for Lig 2 conditions.

The S/G ratio decreased after treatment under oxidizing conditions, meaning that syringyl units are easier to degrade than guaiacyl units. As observed in fig 1, syringyl units are linked to lignin through ether linkages whereas coniferyl units are linked by ethers and 5-5' linkages, which are harder to break under oxidizing conditions.

### **Spectroscopic characterization of lignin**

Lignin and residual lignin were characterized by ATR-IR (Figure 5) in order to identify any changes in the chemical structure of lignin due to the pretreatment conditions or oxidation reactions. The spectra of the pretreated lignin samples (Lig 2, Lig 8 and Lig 22) showed the characteristic bands assigned to lignin structure. The bands were assigned to their corresponding functional groups as described in Table 7.

According to the ATR-IR spectra, pre-treatment conditions did not affect the chemical functionality observed in the lignins. However, when each lignin was compared to the corresponding residual lignin after oxidation, in both cases some changes were observed that are related to the oxidation of the groups present in lignin. The stretch at  $1703\text{ cm}^{-1}$  was slightly displaced to a higher wavenumber with an increase in intensity, primarily due to the formation of carboxylic acids and esters. Also a new band appeared at  $1369\text{ cm}^{-1}$  which was assigned to the aliphatic CH stretch found exclusively in aliphatic methyl groups and OH stretches in phenols. Finally a significant relative decrease in intensity of the band at  $1100\text{ cm}^{-1}$  was observed and assigned to the combination between syringyl and guaiacyl rings which agrees with the decrease of S/G ratio after oxidation measured by py-GCMS<sup>23,24</sup>.

Pyrolysis

The pretreated and oxidized lignin samples were subjected to py-GCMS. The pretreated lignin showed the same peaks in the chromatogram so they were composed of the same fractions but with different relative abundance (Figure 6). As was mentioned in the initial part of the discussion, the chromatograms of the lignins can be divided in three parts (Table 4). Lig 22 showed a higher proportion of fatty acids whereas Lig 8 showed a higher proportion of sugar derived fractions. However for all lignin samples the phenolic and aromatic peaks were the most intense. When the lignin samples were subjected to oxidation it was observed that through the use of hydrogen peroxide without added catalyst, both the sugar and phenolic components degraded approximately in the same proportion. However, with  $\text{TiO}_2/\text{H}_2\text{O}_2$  the phenolic signals were less intense than the sugar signals, which could mean that the phenolic components were degraded selectively by the action of  $\text{TiO}_2$ .

## HPSEC

The  $M_w$  of the obtained lignin and residual lignin samples were measured by HPSEC. The obtained results are detailed in Table 9 and MWD profiles are depicted in Figure 7. Comparing MWD of the lignin samples obtained from different pretreatment conditions, it was observed that they had the same profile but were displaced to longer retention times, which means lower  $M_w$  as shown in Table 9. In accordance with the integrated results, higher reaction time leads to a higher  $M_w$ , which can be due to the self-condensation of lignin or due to interactions with the IL since longer reaction times promote lignin reactivity with the IL anion<sup>25,26</sup>. All lignin samples were degraded after oxidation, with both the catalyzed and uncatalyzed conditions. The extent of degradation was generally higher for Lig 22. Comparing both conditions, the degradation was observed to be higher for  $\text{TiO}_2$  catalyzed conditions for Lig 2 and Lig 22 but not for Lig 8. The obtained residual lignins showed high polydispersity<sup>27,28</sup>.

## Oil Characterization

The oils were characterized by GC-MS, the chromatograms showed a complex mixture of aromatic products derived from lignin with some sugar derived compounds (Figure 8, Figure 9). Several monomers were determined quantitatively, and vanillic acid was the main product of the oils (Table 10). Oxidation with both  $\text{H}_2\text{O}_2$  and  $\text{TiO}_2/\text{H}_2\text{O}_2$  treatments leads to overoxidation to the acid with no selectivity observed towards the aldehyde. Butanoic acid and pentanoic acids were obtained as the main products from hemicellulose, whilst a range of substituted benzoic acids was obtained from lignin as well as the calibrated benzoic acid (Table 11). The presence of fatty acids was also observed. Comparing oxidation treatments, it was observed that the oil obtained with  $\text{H}_2\text{O}_2$  without added catalyst showed higher concentrations of sugar derived acids. However, as Lig 22 showed high concentrations of fatty acids (as observed by py-GCMS), oil 22 is a response of the initial composition of Lig 22 showing high concentration of fatty acids with  $\text{H}_2\text{O}_2$  alone, but with  $\text{TiO}_2/\text{H}_2\text{O}_2$  it showed higher concentrations of phenolics, suggesting that phenolics were oxidising first followed by fatty acids. For oils 8 and 22 obtained with  $\text{TiO}_2/\text{H}_2\text{O}_2$  the main peak of the chromatogram was assigned to 1-(2,4,5-trihydroxyphenyl)-1-butanone, whereas for oil 2 the main peak was assigned to butylated hydroxytoluene, an impurity from the solvent. It was observed that the relative abundance for butylated hydroxytoluene in oil 8 and 22 was 7 % and 6 % respectively. As the concentration is the same for all the samples, the proportion of compounds derived from lignin depolymerization was higher in oil 8 and oil 22 than in oil 2. For oils obtained with  $\text{H}_2\text{O}_2$  alone the main product was pentanoic acid for oil 2 and the proportion of pentanoic acid, 1-(2,4,5-trihydroxyphenyl)-1-butanone and butylated hydroxytoluene was similar in oil 8, whereas oil 22 was composed mainly of butylated hydroxytoluene and fatty acids. In summary, both oil 8 and oil 22 obtained with  $\text{TiO}_2/\text{H}_2\text{O}_2$  showed a higher concentration of lignin derived compounds<sup>29-31</sup>.

## **Ionic liquid characterization**

### **Spectroscopic characterization**

The IL was characterized by ATR-IR before and after pre-treatment and oxidation (Figure 10, Figure 11). ATR-IR spectra of [Et<sub>3</sub>NH][HSO<sub>4</sub>] did not show evidence of moisture contamination and observed bands were assigned to the different groups present in [Et<sub>3</sub>NH][HSO<sub>4</sub>] structure. Bands at 3037, 2998, 2951, 2888, 2818, 2717, 2558 and 2505 cm<sup>-1</sup> were assigned to asymmetric and symmetric stretching vibrations of CH<sub>2</sub> and CH<sub>3</sub> on the ammonium salt, the band at 1478 cm<sup>-1</sup> was assigned to the NH deformation vibration, the band at 1440 cm<sup>-1</sup> was assigned to the S-CH<sub>3</sub> asymmetric deformation vibration, bands at 1401, 1291, 1233, 1061 and 1034 cm<sup>-1</sup> were assigned to the HOSO<sub>3</sub><sup>-</sup> asymmetric and symmetric stretching vibrations, the band at 1364 cm<sup>-1</sup> was assigned to alkyl chain deformation on the ammonium salt and the band at 838 cm<sup>-1</sup> corresponded to CH in plane vibration. These bands are modified only by the addition of water to the IL, whereby some bands assigned to the anion overlapped with adjacent bands. The bands at 1289 and 1233 cm<sup>-1</sup> overlapped with the band at 1149 cm<sup>-1</sup> and the band at 1062 cm<sup>-1</sup> overlapped with the band at 1031 cm<sup>-1</sup>, all of these bands were assigned to HOSO<sub>3</sub><sup>-</sup><sup>32,33</sup>. A new band was also observed at 1644 cm<sup>-1</sup> and was assigned to water itself. Taking into account that the IL is mixed with water during pre-treatment to establish whether the IL was contaminated by biomass waste, the obtained spectra were compared with the spectrum from the IL and water mixture. The only difference observed among the spectra of the IL after pre-treatment and oxidation, was the appearance of a new band at 1731 cm<sup>-1</sup>, which increases in intensity with increased pre-treatment time. Moreover, after oxidation using TiO<sub>2</sub>/H<sub>2</sub>O<sub>2</sub> the intensity of the band was comparatively higher than for oxidation with H<sub>2</sub>O<sub>2</sub> alone. This band was assigned to the C=O of the acetate group, which is formed during the degradation stages of hemicellulose. As this band is more intense for TiO<sub>2</sub>/H<sub>2</sub>O<sub>2</sub> samples it is postulated that hemicelluloses are not completely degraded to CO<sub>2</sub> and

H<sub>2</sub>O, as happens with H<sub>2</sub>O<sub>2</sub> alone where release of pressure was observed when the tube was opened after the treatment, which cannot be due to IL as it has low vapor pressure nor water as it was opened at room temperature. The acetic acid was not extracted by MeTHF and remained in the IL<sup>34,35</sup>.

### **HPLC characterization**

[Et<sub>3</sub>NH][HSO<sub>4</sub>] was characterized by HPLC to determine the impurities which remained after oxidation. As observed in the chromatograms (Figure 12), after pre-treatment some impurities remained in solution after lignin precipitation. After oxidation via both homogeneous and heterogeneous conditions, the chromatogram only showed one small peak apart from the one assigned to [Et<sub>3</sub>NH][HSO<sub>4</sub>]. After oxidation and extraction processes [Et<sub>3</sub>NH][HSO<sub>4</sub>] was also purified and was ready to be reused.

### **Conclusion**

Resolution willow specie was chosen as best source of lignin for being depolymerized. Pre-treatment conditions had no influence on lignin solubility and recovery but affected the further reactivity of lignin as its composition was different as well as its M<sub>w</sub>. Lignin was successfully depolymerized under oxidizing conditions either with H<sub>2</sub>O<sub>2</sub> or TiO<sub>2</sub>/H<sub>2</sub>O<sub>2</sub> treatments. However whilst the composition of the obtained oils was different, oxidation via hydrogen peroxide alone leads to an oil rich in sugar derived acids whereas oxidation with TiO<sub>2</sub> catalysis leads to an oil rich in phenolic derived fragments, derived from lignin. The addition of TiO<sub>2</sub> enhanced the selectivity of the reaction and the yields of phenolic monomers, the main target when lignin is depolymerizing.

### **References**



- 01, Zhang, Y.H.P.; Ding, J.R.; Mielenz, S.Y.; Cui, J.B.; Elander, R.T.; Laser M.; Himmel, M.E.; McMillan, J.R.; Lynd, L.R. Fractionating Recalcitrant Lignocellulose at Modest Reaction Conditions. *Biotechnol. Bioeng.* 2007, **97**, 214-223.
- 02, Fang, Z.; Fang, C. "Complete dissolution and hydrolysis of wood in hot water." *Aichen J.* 2008, **54**, 2751-2758.
- 03, Garcia, A.; Toledano, A.; Serrano, L.; Egües, I.; Gonzalez, M.; Martín, F.; Labidi, J.. Characterization of lignins obtained by selective precipitation. *Sep. Purif. Technol.* 2009, **68**, 193-198.
- 04, Kilpeläinen, I.; Xie, H.; King, A.; Granstrom, M.; Heikkinen, S.; Argyropoulos, D.S.. Disolution of wood in ionic liquids. *J. Agric. Food Chem.* 2007, **55**, 9142-9148.
- 05, Yang, D.; Qiu, X.; Zhou, M.; Lou, H. Properties of sodium lignosulfonate as dispersant of coal water slurry. *Energy Convers. Manage.* 2007, **48**, 2433–2438.
- 06, Sena-Martins, G.; Almeida-Vara, E.; Duarte, J.C. Eco-friendly new products from enzymatically modified. *Ind. Crops Prod.* 2008, **27**, 189–195.
- 07, Agrwal, A.; Kaushik, N.; Biswas, S. Derivatives and Applications of Lignin – An Insight. *the scitech journal.* 2014, **1** (7), 30-36.
- 08, Thakur, V. K.; Thakur, M. K.; Raghavan, P.; Kessler M. R. Progress in Green Polymer Composites from Lignin for Multifunctional Applications: A Review. *ACS. Sust. Chem. Eng.* 2014, **2**, 1072-1092.
- 09, ESCOP. *Willow varietal identification Guide.* Carlow: teagasc.n.d. **1997**.
- 10, Plechkova, N.V.; Seddon, K.R. Application of IL in the chemical industry. *Chem. Soc. Rev.* 2008, **37**, 123-150.
- 11, Seddon, R.D.; Rogerds, K.R. Ionic Liquids- solvents of the future. *Science.* 2003, **302**, 792-793.

- 12, Marszall, M. P.; Kaliszan, R. Application of ionic liquids in liquid chromatography. *Crit. Rev. Anal. Chem.* 2007, **37**, 127-140.
- 13, Nockemann, P.; Binnemans, K.; Driesen, K. Purification of imidazolium ionic liquids for spectroscopic applications. *Chem. Phys. Lett.* 2005, **415**, 131-136.
- 14, MacFarlane, D. R.; Tachikawa, N.; Forsyth, M.; Pringle, J. M.; Howlett, P.C.; Elliott, G. D.; Davis, J. H.; Watanabe, M.; Simon, P.; Angell, A. Energy applications of ionic liquids. *Energy Environ. Sci.* 2014, **7**, 232-250.
- 15, Xu, C.; Arancon, R. A. D.; Labidi, L.; Luque, R.; Lignin depolymerization strategies: towards valuable chemicals and fuels. *Chem. Soc. Rev.* 2014, **43**, 7485-7500.
- 16, Tan, S. S. Y.; MacFarlane, D. R.; Upfal, J.; Edye, L. A.; Doherty, W. O. S.; Patti, A. F.; Pringle, J. M.; Scott, J. L. Extraction of lignin from lignocellulose at atmospheric pressure using alkylbenzenesulfonate ionic liquid. *Green Chem.* 2009, **11**, 339-345.
- 17, George, A.; Tran, K.; Morgan, T. J.; Benke, P. I.; Berrueco, C.; Lorente, E.; Wu, B. C.; Keasling, J. D.; Simmons, B. A.; Holmes, B. M. The effect of ionic liquid cation and anion combinations on the macromolecular structure of lignins. *Green Chem.* 2011, **13**, 3375-3385.
- 18, Behling, R.; Valange, S.; Chatel, G.; Heterogeneous catalytic oxidation for lignin valorization into valuable chemicals: what results? What limitations? What trends? *Green Chem.* 2016, **18**, 1839-1854.
- 19, Ma, R.; Xu, Y.; Zhang, X. Catalytic oxidation of biorefinery lignin to value-added chemicals to support sustainable biofuel production. *Chem. Sus. Chem.* 2015, **8**, 24-51.
- 20, Chatel, G.; Rogers, R. D. Review: Oxidation of lignin using ionic liquids-an innovative strategy to produce renewable chemicals. *ACS Sustainable Chem. Eng.* 2013, **2** (3), 322-339.
- 21, Prado, R.; Brandt, A.; Erdocia, X.; Hallett, J.; Welton, T.; Labidi, J. Lignin oxidation and depolymerisation in ionic liquids. *Green Chem.* 2016, **18**, 834-841.

- 22, Verdia, P.; Brandt, A.; Hallett, J. P.; Ray, M. J.; Welton, T. Fractionation of lignocellulosic biomass with the ionic liquid 1-butylimidazolium hydrogen sulfate. *Green Chem.* 2014, **16**, 1617-1627.
- 23, García, A.; Toledano, A.; Serrano, L.; Egüés, I.; González, M.; Martín, F.; Labidi, J.. Characterization of lignins obtained by selective precipitation. *Sep. Purif. Technol.* 2010, **68**, 193-198.
- 24, Lau, S.; Ibrahim, R. FT-IR spectroscopic studies on lignin from some tropical woods and rattan. *Pertanika.* 1992, **14** (1), 78-81.
- 25, Yinghuai, Z.; Yuanting, K. T.; Hosmane, N. S. Applications of Ionic Liquids in Lignin Chemistry,. *Ionic Liquids - New Aspects for the Future*. Edited by J. Kadokawa. Intech. doi:10.5772/51161. 2013
- 26, Pu, Y.; Jiang, N.; Ragauskas, A.J.; Ionic liquid as a green solvent for lignin. *J. Wood Chem. Technol.* 2007, **27**, 23-33.
- 27, Buranov, A.U.; Ross, K.A.; Mazza, G. Isolation and characterization of lignins extracted from flax shives using. *Bioresour. Technol.* 2010, **101**, 7446–7455.
- 28, El Hage, R.; Brosse, N.; Chrusciel, L.; Sanchez, C.; Sannigrahi, P.; Ragauskas, A. Characterization of milled wood lignin and ethanol organosolv lignin from miscanthus. *Polym. Degrad. Stab.* 2009, **94**, 1632-1638.
- 29, Lanzalunga, O.; Bietti, M. Photo- and radiation chemical induced degradation of lignin model compounds. *J. Photochem. Photobiol. B.* 2000, **56**, 85-108.
- 30, Toledano, A.; Serrano, L.; Pineda, A.; Romero, A. A.; Luque, R.; Labidi, J. Microwave-assisted depolymerisation of organosolv lignin via mild hydrogen-free hydrogenolysis: Catalyst screening. *Appl. Catal. B.* 2014, **145**, 43-55.
- 31, Pandey, M. P.; Kim, C. S. “Lignin depolymerization and conversion: a review of thermochemical methods.” *Chem. Eng. Technol.* 2011, **34**, 29-41.

32, Shi, F.; Deng, Y. Abnormal FT-IR and FT-Raman spectra of ionic liquids. *Spectrochim. Acta A*. 2005, **62**, 239-244.

33, Pretsch, E.; Bühlmann, P.; Affolter, C.; Herrera, A.; Martínez, A. *Structure determination of organic compounds*. New York: Springer-Verlag. 2000

34, Fanf, J. M.; Sun, R. C.; Tomkinson, J. Isolation and characterization of hemicelluloses. *Cellulose*. 2000, **7**, 87-107.

35, Peng, F.; Bian, J.; Peng, P.; Guan, Y.; Xu, F.; Sun, R.C.; Fractional separation and structural features of hemicelluloses from sweet sorghum leaves. *Bioresource*. 2012, **7** (4) 4744-4759.

## List of tables

*Table 1: Different willow lignin properties*

*Table 2: Assignments of  $^{13}\text{C}$ - $^1\text{H}$  cross signals in the (HSQC) of lignin and fibres*

*Table 3: HSQC-NMR characterization of different species*

*Table 4: py-GCMS determined compounds*

*Table 5: Pre-treatment yields*

*Table 6: Yields after oxidation of lignin*

*Table 7: ATR-Ir band assignment*

*Table 8: py-GCMS identified compounds of Lignin*

*Table 9: HPSEC results for lignins*

*Table 10: Phenolic calibrated compounds determined by GCMS*

*Table 11: Oil composition non calibrated compounds identified by GCMS*

Table 1: Different willow lignin properties

Sample name	Pre-treatment	Lignin yield	S/G py-GCMS	M <sub>w</sub>	Polydispersity
Resolution	22 h at 120 °C	20±1	1.35±0.08	35111	13.50
Terranova	22 h at 120 °C	18.83±0.9	1.92±0.06	48056	16.67
Endurance	22 h at 120 °C	17.8±0.8	1.56±0.1	70456	31.58

Table 2: Assignments of <sup>13</sup>C-1H cross signals in the (HSQC) of lignin and fibres

Lable	δ <sub>C</sub> /δ <sub>H</sub> (ppm)	Assignments
	56.359/3.759	C-H in methoxyls groups
A	59.777/3.257	C <sub>γ</sub> -H <sub>γ</sub> in β-O-4' substructures
	60.538/3.661	
	60.305/4.051	
A'	63.017/3.693	C <sub>γ</sub> -H <sub>γ</sub> in β-O-4' substructures
A	71.657/4.181	C <sub>α</sub> -H <sub>α</sub> in β-O-4 linked to a G unit
A	71.657/3.804	C <sub>α</sub> -H <sub>α</sub> in β-O-4
A	72.241/4.866	C <sub>α</sub> -H <sub>α</sub> in β-O-4 linked to a S unit
A	85.662/4.632	C <sub>α</sub> -H <sub>α</sub> in resinol structure
B	86.747/4.092	C <sub>β</sub> -H <sub>β</sub> in β-O-4 in dibenzodiocoxin
C	87.540/5.449	C <sub>α</sub> -H <sub>α</sub> in resinol structure
S	104.273/6.616	C <sub>2,6</sub> -H <sub>2,6</sub> in S units
S'	106.967/7.334	C <sub>2,6</sub> -H <sub>2,6</sub> in oxidized (C <sub>α</sub> =O) S units
E	110.957/7.378	C <sub>8</sub> -H <sub>8</sub> in p-coumarate
	112.691/6.656	
G	110.458/7.157	C <sub>2</sub> -H <sub>2</sub> in guaiacyl units
G'	111.195/6.919	C <sub>2</sub> -H <sub>2</sub> in oxidised guaiacyl units
G	115.754/6.762	C <sub>5</sub> -H <sub>5</sub> in guaiacyl units
E	115.959/6.261	C <sub>3,5</sub> -H <sub>3,5</sub> in p-coumarate
E	126.927/6.993	C <sub>β</sub> -H <sub>β</sub> in cinnamyl aldehyde end groups
F	131.332/7.627	C <sub>2,6</sub> -H <sub>2,6</sub> in p-hydroxybenzoate substructures

Table 3: HSQC-NMR characterization of different species

	S/G NMR	MeOH	β-O-4
Resolution	1.16	12.81	1.77
Terranova	1.71	10.50	1.27
Endurance	1.40	9.21	1.40

Table 4: py-GCMS determined compounds

<b>r.t</b>	<b>Fraction</b>	<b>Resolution</b>	<b>Terranova</b>	<b>Endurance</b>
<b>4.311</b>	1-(2-Phenylsulfanyl-ethyl)-pyrrolidine	X		
<b>4.594</b>	1H-Pyrrole, 1-ethyl-	X	X	X
<b>4.854</b>	Furfural	X	X	X
<b>5.501</b>	Thiophene		X	X
<b>7.014</b>	2-Furancarboxaldehyde, 5-methyl-	X		
<b>7.26</b>	Phenol	X	X	X
<b>7.655</b>	Acetamide, N,N-diethyl-	X	X	
<b>8.192</b>	Benzyl Alcohol	X		
<b>9.116</b>	Phenol, 2-methoxy- (guaiacol)	X	X	X
<b>9.497</b>	2-Furanmethanol	X		
<b>9.509</b>	Phenol, 3,4,5-trimethyl-	X		
<b>9.607</b>	Levoglucosenone		X	X
<b>9.859</b>	2,5-Pyrrolidinedione, 1-ethyl-	X		
<b>10.243</b>	Benzene, 1-ethenyl-4-methoxy-	X		
<b>10.422</b>	Phenol, 4-ethyl-	X		
<b>11.085</b>	Phenol, 2-methoxy-4-methyl-	X		
<b>11.421</b>	1,4:3,6-Dianhydro-.alpha.-d-glucopyranose	X	X	X
<b>11.548</b>	Benzofuran, 2,3-dihydro-	X	X	
<b>13.442</b>	Phenol, 4-ethyl-2-methoxy-	X		
<b>14.608</b>	2-Methoxy-4-vinylphenol	X	X	X
<b>15.683</b>	Phenol, 2,6-dimethoxy- (syringol)	X	X	X
<b>16.878</b>	Vanillin	X	X	
<b>17.895</b>	Benzoic acid, 4-hydroxy-3-methoxy-	X	X	X
<b>17.964</b>	Phenol, 2-methoxy-4-(1-propenyl)-	X	X	
<b>18.38</b>	1-Decene	X		
<b>18.669</b>	Ethanone, 1-(4-hydroxy-3-methoxyphenyl)	X	X	
<b>19.079</b>	Phenol, 2,4-bis(1,1-dimethylethyl)	X		
<b>19.356</b>	Ethanone, 1-(2,6-dihydroxy-4-methoxyphenyl)-	X	X	
<b>19.448</b>	Homovanillyl alcohol	X	X	X
<b>19.985</b>	Ethanone, 1-(3,4-dimethoxyphenyl)-	X		
<b>20.101</b>	2,5-dimethoxy-4-ethylamphetamine		X	X
<b>20.343</b>	2,4'-Dihydroxy-3'-methoxyacetophenone	X	X	X
<b>20.442</b>	Diethyl Phthalate	X	X	
<b>20.563</b>	Phenol, 2,6-dimethoxy-4-(2-propenyl)-	X		

<b>21.255</b>	Phenol, 2,6-dimethoxy-4-(2-propenyl)-	X		
<b>21.655</b>	Cyclododecane	X		
<b>21.909</b>	Phenol, 2,6-dimethoxy-4-(2-propenyl)-	X	X	X
<b>22.324</b>	Ethanone, 1-(4-hydroxy-3,5-dimethoxyphenyl)-	X	X	X
<b>22.775</b>	Desaspidinol	X	X	X
<b>23.069</b>	Aspidinol			X
<b>23.526</b>	4-dimethylamino salicylic acid		X	X
<b>23.959</b>	Benzaldehyde, 2-hydroxy-4-(phenylmethoxy)-	X	X	
<b>24.504</b>	Hexadecanoic acid, methyl ester	X	X	
<b>24.773</b>	n-Hexadecanoic acid		X	X
<b>24.975</b>	n-Hexadecanoic acid		X	X
<b>25.097</b>	Hexadecanoic acid, ethyl ester	X	X	X
<b>26.200</b>	9,12-Octadecadienoic acid			X
<b>26.714</b>	Linoleic acid ethyl ester	X	X	X
<b>27.066</b>	Octadecanoic acid		X	X
<b>27.950</b>	Tricosane			X
<b>28.325</b>	6,6-Dimethylhepta-2,4-diene			X
<b>28.515</b>	Dodecamide, N,N-diethyl		X	X
<b>28.550</b>	1-Phenanthrenecarboxylic acid, 1,2,3,4,4a,9,10,10a-octahydro-1,4a-dimethyl-7-(1-methylethyl)-, methyl ester, [1R-(1.alpha.,4a.beta.,10a.alpha.)]-			X
<b>28.793</b>	Tetracosane			X
<b>29.601</b>	Pentacosane			X
<b>29.965</b>	1,2-Benzenedicarboxylic acid, mono (2-ethylhexyl) ester	X	X	X
<b>30.254</b>	Decosanoic acid, ethyl ester	X		
<b>30.375</b>	Eicosane			X
<b>31.218</b>	Octadecane		X	X
<b>32.206</b>	Octadecane			X
<b>33.361</b>	Nonacosane			X
<b>36.613</b>	Stigmastan-3,5-diene	X	X	X

Table 5: Pre-treatment yields

Sample name	Pre-treatment	Solved biomass %	Lignin yield %	Char %	Residual Lignin %	S/G
<b>Lig 2</b>	2 h at 150 °C	60±1	20±1	56±1	40.3±0.9	2.16±0.08



<b>Lig 8</b>	8 h at 120 °C	61.0±0.9	19.7±0.3	56.6±0.5	39.5±0.7	2.2±0.1
<b>Lig 22</b>	22 h at 120 °C	64.2±0.6	20.1±0.4	11.8±0.2	61.3±0.5	2.26±0.06

Table 6: Yields after oxidation of lignin

Sample	Lignin %	Oil %	S/G
<b>Lig 2</b>	20 ± 1		2.16±0.08
<b>Lig 2 H<sub>2</sub>O<sub>2</sub></b>	7.6 ± 0.4	15.9 ± 0.6	1.62
<b>Lig 2 TiO<sub>2</sub>/H<sub>2</sub>O<sub>2</sub></b>	2.6 ± 1	22.3 ± 0.4	1.71
<b>Lig 8</b>	19.7± 0.3		2.2±0.1
<b>Lig 8 H<sub>2</sub>O<sub>2</sub></b>	6.3 ± 0.4	14.9 ± 0.8	1.71
<b>Lig 8 TiO<sub>2</sub>/H<sub>2</sub>O<sub>2</sub></b>	5.4 ± 0.1	16.3 ± 0.7	1.83
<b>Lig 22</b>	20.1 ± 0.6		2.26±0.06
<b>Lig 22 H<sub>2</sub>O<sub>2</sub></b>	5.35 ±0.05	6.9 ± 0.2	1.18
<b>Lig 22 TiO<sub>2</sub>/H<sub>2</sub>O<sub>2</sub></b>	2 ± 1	11.10 ±0.7	1.16

Table 7: ATR-IR band assignment

Band cm <sup>-1</sup>	Functional group
<b>3346</b>	–OH stretch
<b>2932</b>	CH stretches in methyl and methylene groups
<b>2851</b>	
<b>1703</b>	C=O stretches in unconjugated ketones, carbonyl and ester groups
<b>1604</b>	Aromatic skeletal vibrations and C=O stretch
<b>1513</b>	Aromatic skeletal vibrations
<b>1454</b>	CH deformation in methyl and methylene groups
<b>1428</b>	Aromatic skeletal vibrations combined with C-H in plane deformation
<b>1209</b>	Guaiacyl ring breathing plus C=O stretch
<b>1110</b>	Etherified guaiacyl ring plus syringyl unit and secondary alcohol plus C=O stretch
<b>1028</b>	C-O deformation in primary alcohol plus C=O stretch in unconjugated ketones and the aromatic C-H in plane deformation
<b>913</b>	C-H out of plane deformation
<b>834</b>	C-H out of plane deformation in 2 and 6 positions on syringyl ring

Table 8: py-GCMS identified compounds of Lignin

<b>r.t</b>	<b>Fraction</b>
<b>4.311</b>	1-(2-Phenylsulfanyl-ethyl)-pyrrolidine
<b>4.594</b>	1H-Pyrrole, 1-ethyl-
<b>4.854</b>	Furfural
<b>7.014</b>	2-Furancarboxaldehyde, 5-methyl-
<b>7.26</b>	Phenol
<b>7.655</b>	Acetamide, N,N-diethyl-
<b>8.192</b>	Benzyl Alcohol
<b>9.116</b>	Phenol, 2-methoxy- (guaiacol)
<b>9.497</b>	2-Furanmethanol
<b>9.509</b>	Phenol, 3,4,5-trimethyl-
<b>9.859</b>	2,5-Pyrrolidinedione, 1-ethyl-
<b>10.243</b>	Benzene, 1-ethenyl-4-methoxy-
<b>10.422</b>	Phenol, 4-ethyl-
<b>11.085</b>	Phenol, 2-methoxy-4-methyl-
<b>11.421</b>	1,4:3,6-Dianhydro- .alpha.-d-glucopyranose
<b>11.548</b>	Benzofuran, 2,3-dihydro-
<b>13.442</b>	Phenol, 4-ethyl-2-methoxy-
<b>14.608</b>	2-Methoxy-4-vinylphenol
<b>15.683</b>	Phenol, 2,6-dimethoxy- (syringol)
<b>16.878</b>	Vanillin
<b>17.895</b>	Benzoic acid, 4-hydroxy-3-methoxy-
<b>17.964</b>	Phenol, 2-methoxy-4-(1-propenyl)-
<b>18.38</b>	1-Decene
<b>18.669</b>	Ethanone, 1-(4-hydroxy-3-methoxyphenyl)
<b>19.079</b>	Phenol, 2,4-bis(1,1-dimethylethyl)
<b>19.356</b>	Ethanone, 1-(2,6-dihydroxy-4-methoxyphenyl)-
<b>19.448</b>	Homovanillyl alcohol
<b>19.985</b>	Ethanone, 1-(3,4-dimethoxyphenyl)-
<b>20.343</b>	2,4'-Dihydroxy-3'-methoxyacetophenone
<b>20.442</b>	Diethyl Phthalate
<b>20.563</b>	Phenol, 2,6-dimethoxy-4-(2-propenyl)-
<b>21.255</b>	Phenol, 2,6-dimethoxy-4-(2-propenyl)-
<b>21.655</b>	Cyclododecane
<b>21.909</b>	Phenol, 2,6-dimethoxy-4-(2-propenyl)-
<b>22.324</b>	Ethanone, 1-(4-hydroxy-3,5-dimethoxyphenyl)-
<b>22.775</b>	Desaspidinol
<b>23.959</b>	Benzaldehyde, 2-hydroxy-4-(phenylmethoxy)-
<b>24.404</b>	Hexadecanoic acid, methyl ester
<b>25.097</b>	Hexadecanoic acid, ethyl ester

<b>26.714</b>	Linoleic acid ethyl ester
<b>29.965</b>	1,2-Benzenedicarboxylic acid, mono (2-ethylhexyl) ester
<b>30.254</b>	Docosanoic acid, ethyl ester
<b>36.613</b>	Stigmastan-3,5-diene

Table 9: HPSEC results for lignins

	<b>Mw</b>	<b>Mn</b>	<b>Polydispersity</b>
<b>Lig 2</b>	19,744	2,001	9.87
<b>Lig 2 H<sub>2</sub>O<sub>2</sub></b>	13,041	1,505	8.66
<b>Lig 2 TiO<sub>2</sub>/H<sub>2</sub>O<sub>2</sub></b>	10,622	1,441	7.37
<b>Lig 8</b>	24,555	2,549	9.63
<b>Lig 8 H<sub>2</sub>O<sub>2</sub></b>	9,820	1,138	8.63
<b>Lig 8 TiO<sub>2</sub>/H<sub>2</sub>O<sub>2</sub></b>	13,612	1,437	9.47
<b>Lig 22</b>	35,111	2,601	13.50
<b>Lig 22 H<sub>2</sub>O<sub>2</sub></b>	8,463	1,091	7.75
<b>Lig 22 TiO<sub>2</sub>/H<sub>2</sub>O<sub>2</sub></b>	5,028	770	6.52

Table 10: Phenolic calibrated compounds determined by GCMS

<b>r.t.</b>	<b>standards</b>	<b>Oil 2 H<sub>2</sub>O<sub>2</sub></b>	<b>Oil 2 TiO<sub>2</sub></b>	<b>Oil 8 H<sub>2</sub>O<sub>2</sub></b>	<b>Oil 8 TiO<sub>2</sub></b>	<b>Oil 22 H<sub>2</sub>O<sub>2</sub></b>	<b>Oil 22 TiO<sub>2</sub></b>
<b>5.57</b>	Phenol (a)	0.07	0.16	0.06	0.06	0.22	0.13
<b>7.27</b>	Guaiacol (b)	0.04	0.11	0.04	0.04	0.12	0.09
<b>9.15</b>	Catechol (c)	0.19	0.49	0.24	0.18	0.58	0.49
<b>10.94</b>	3-methoxycatechol (d)	0.23	0.27	0.13	0.15	0.22	0.24
<b>11.71</b>	4-methylcatechol (e)	0.03	0.02	0.02	0.02	0.00	0.00
<b>13.71</b>	Syringol (f)	0.06	0.15	0.08	0.06	0.06	0.11
<b>14.90</b>	Vanillin (g)	0.00	0.00	0.00	0.00	0.00	0.01
<b>16.77</b>	Acetovanillone (h)	0.00	0.01	0.00	0.01	0.03	0.01
<b>18.02</b>	Vanillic acid (3-Hydroxy-4-methoxy benzoic acid) (i)	27.92	39.72	31.71	14.25	32.96	43.41
<b>17.47</b>	4-hydroxy-3-methoxyphenil (j)	0.00	0.01	0.03	0.03	0.00	0.01
<b>20.33</b>	Acetosyringone (k)	0.00	0.01	0.00	0.00	0.00	0.01

Table 11: Oil composition non calibrated compounds identified by GCMS

<b>n</b>	<b>Non calibrated compounds</b>
1	Maleic anhydride
2	2(3H)-Furanone, 5-methyl-
3	Butyrolactone
4	Butanoic acid, 3-hydroxy-, ethyl ester
5	2(3H)-Furanone, dihydro-5-methyl-
6	Ethylene glycol diglycidyl ether
7	Succinic anhydride
8	2-Furancarboxylic acid, ethyl este
9	Pentanoic acid, 4-oxo-, ethyl este
10	Pentanoic acid, 4-oxo-
11	Butanedioic acid, ethyl methyl ester
12	4-Isopropylbenzenethiol, S-methyl
13	Ethyl hydrogen succinate
14	Butanedioic acid, diethyl ester
15	Ethyl hydrogen fumarate
16	Acetic acid, 2-phenylethyl ester
17	Salicylic acid
18	1-Methyl-3-piperidinemethanol
19	2,5-Cyclohexadiene-1,4-dione, 2,6-bis(1,1-dimethylethyl)-
20	Butylated Hydroxytoluene
21	1,2-Dimethoxy-4-(2-propenyloxy)benzene
22	1-Butanone, 1-(2,4,5-trihydroxyphenyl)-
23	Benzoic acid, 4-hydroxy-3-methoxy-
24	Naphthalene, 1-isocyanato-
25	Pentanoic acid, 4-oxo-, phenylmethyl ester
26	Azelaic Acid
27	3-Methoxydiphenylamine
28	Benzoic acid, 4-hydroxy-3,5-dimethoxy
29	Benzoic acid, 2-hydroxy-, phenylmethyl ester
30	Hexadecanoic acid, ethyl ester
31	Octadecanoic acid, ethyl ester
32	(E)-9-Octadecenoic acid ethyl este
33	Octadecanoic acid, 2-(acetyloxy)-1 - [(acetyloxy)methyl]ethyl ester

## List of figures

*Figure 1: a) MWD of different species b) py-GCMS Chromatogram of the different species*

*Figure 2: Lignin structure*

*Figure 3: HSQC-NMR spectra of the different species a) Resolution, b) Terranova, c) Endurance*

*Figure 4: Lignin detected structures*

*Figure 5: ATR-IR of lignin and residual lignin*

*Figure 6: py-GCMS chromatograms of different samples*

*Figure 7: MWD of different lignins*

*Figure 8: oil Chromatogram*

*Figure 9: Oil chromatograms obtained by GCMS*

*Figure 10: ATR-IR spectra of the IL and its mixture with water*

*Figure 11: ATR-IR spectra of IL after the different treatments*

*Figure 12: HPLC results for IL after the different conditions a) after pretreatment b) after treatment with H<sub>2</sub>O<sub>2</sub> alone c) after treatment with TiO<sub>2</sub>/H<sub>2</sub>O<sub>2</sub>*

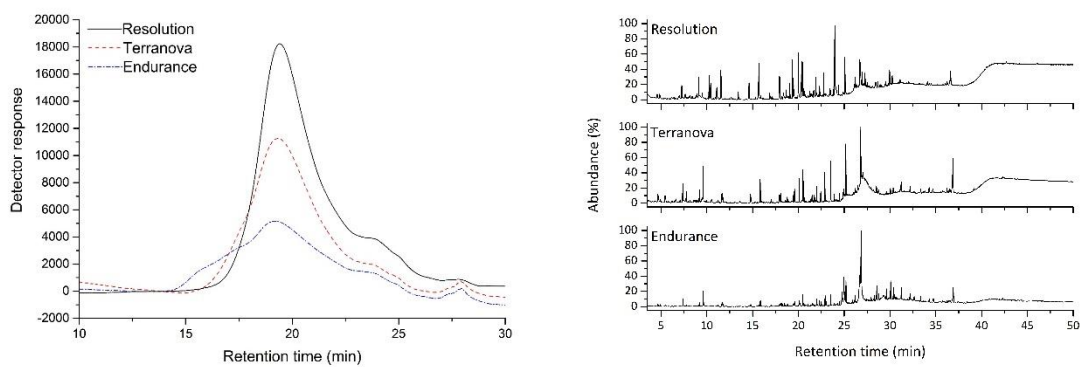


Figure 1: a) MWD of different species b) py-GCMS Chromatogram of the different species

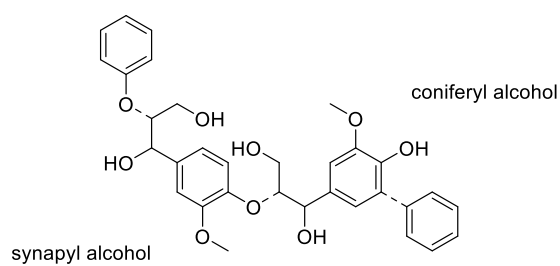


Figure 2: Lignin structure

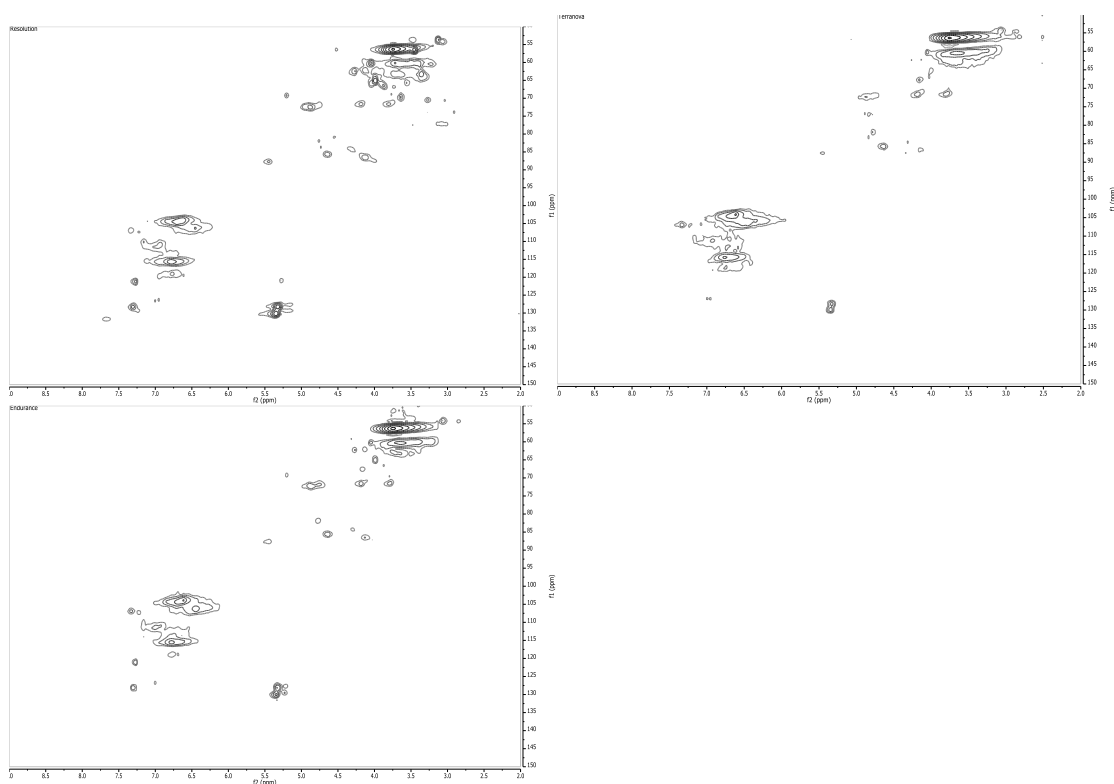


Figure 3: HSQC-NMR spectra of the different species a) Resolution, b) Terranova, c) Endurance

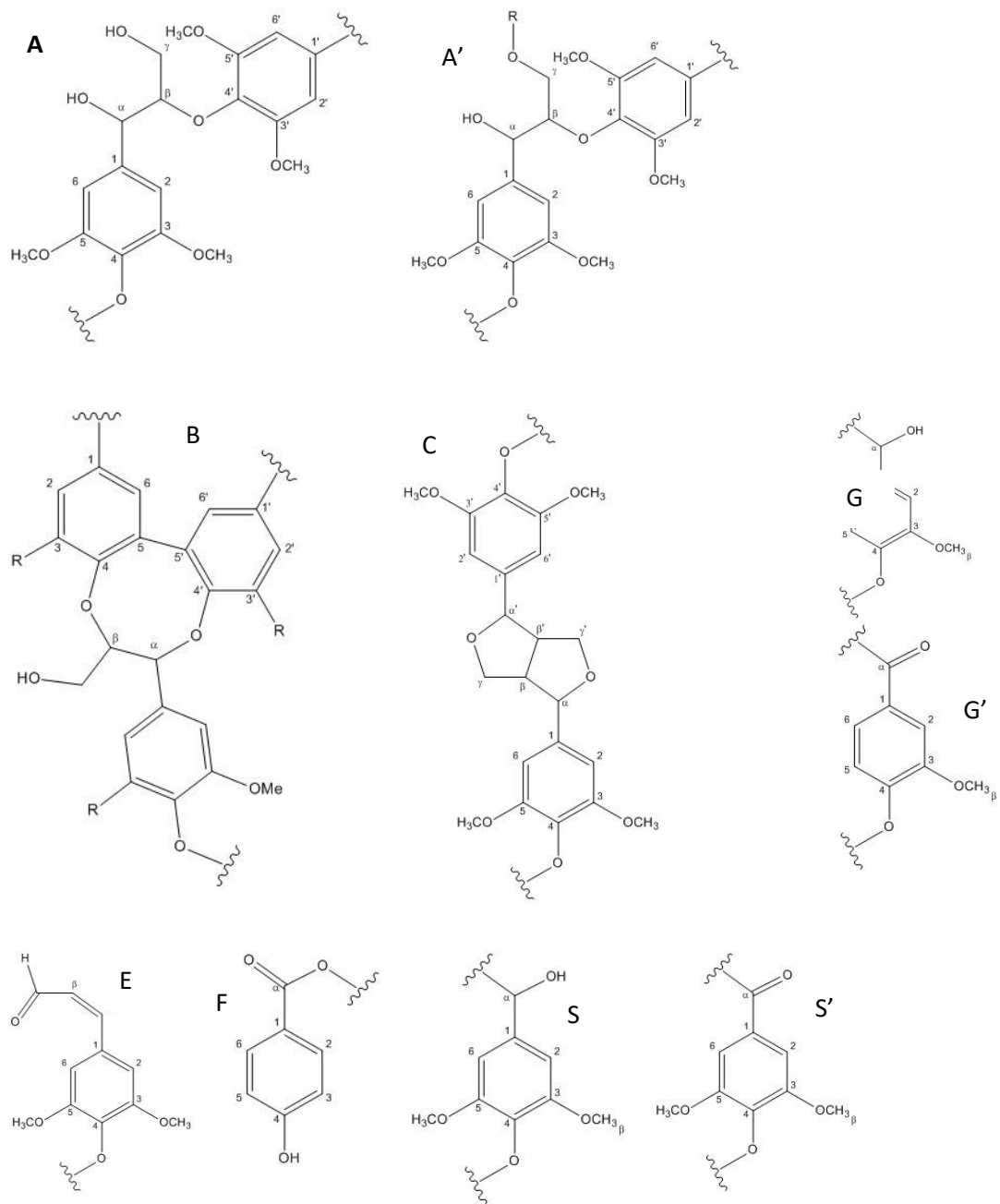


Figure 4: Lignin detected structures

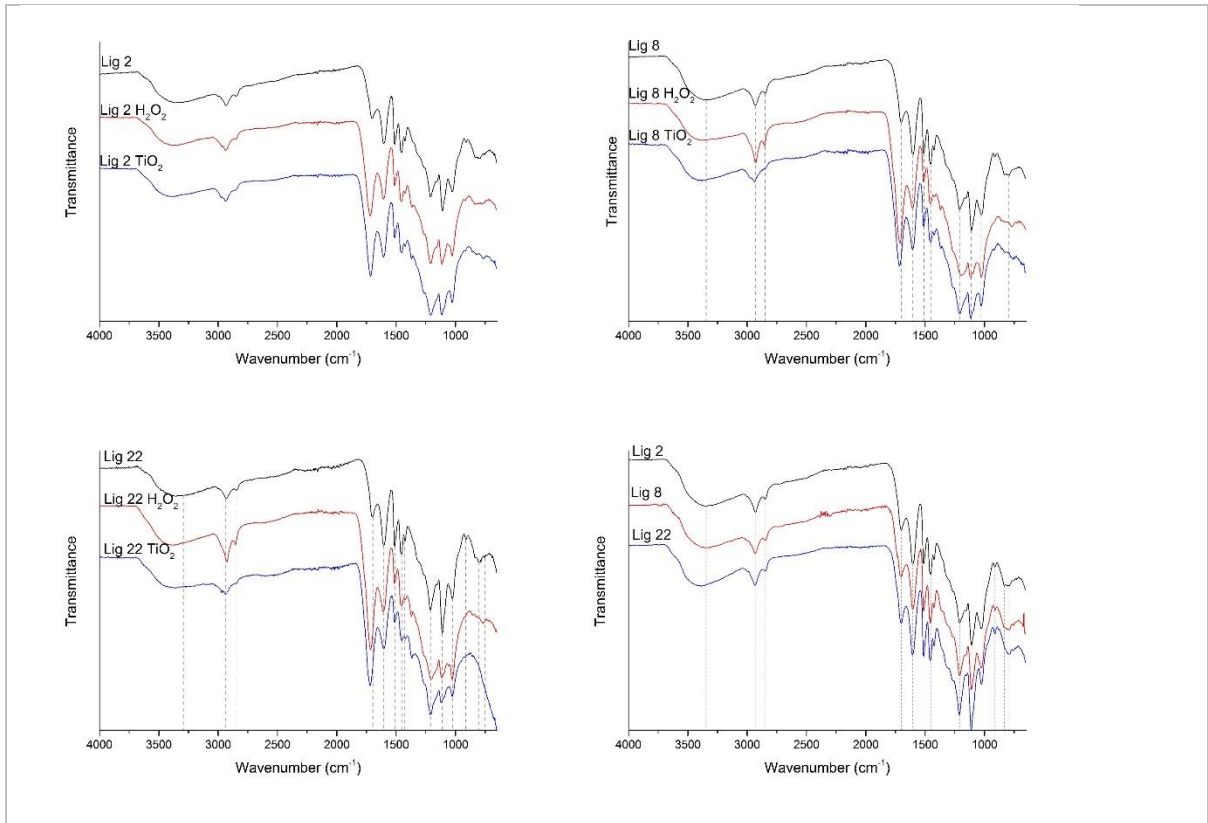


Figure 5: ATR-IR of lignin and residual lignin



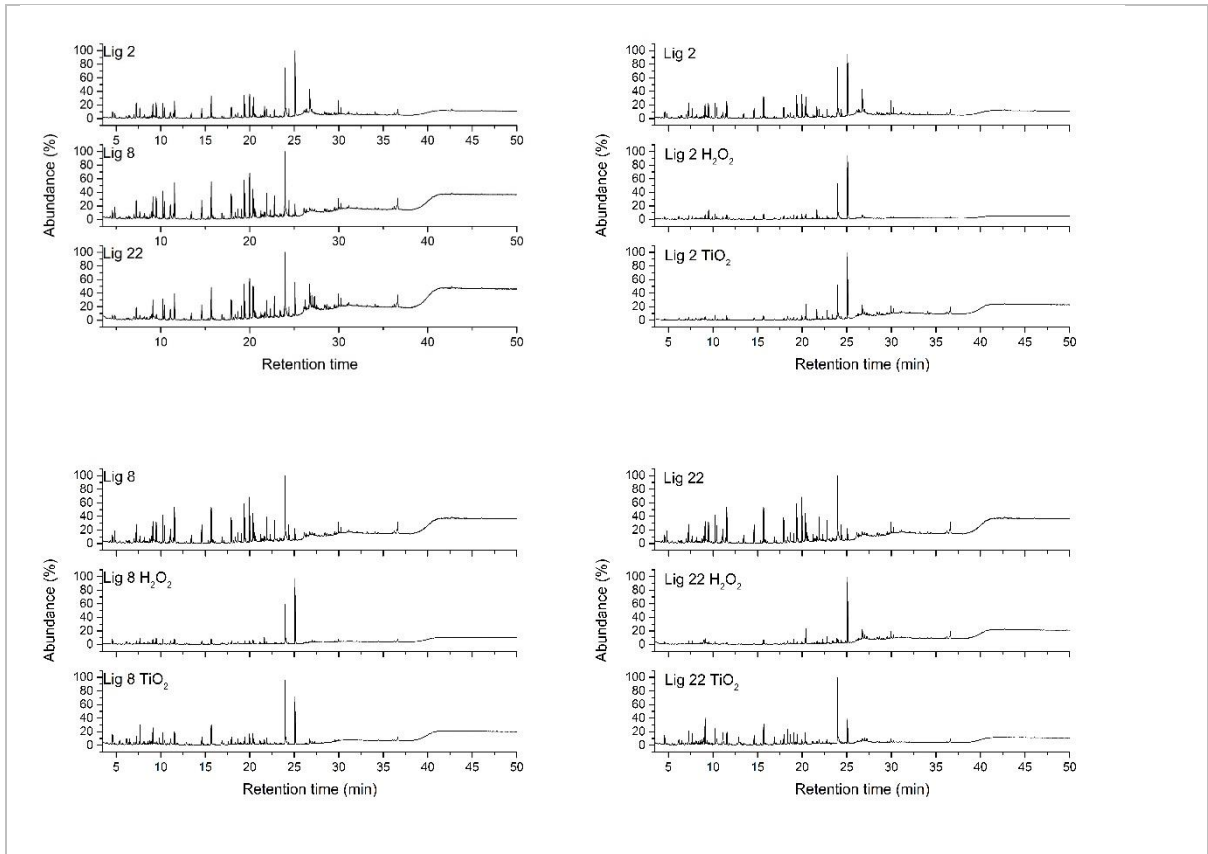


Figure 6: *py-GCMS chromatograms of different samples*

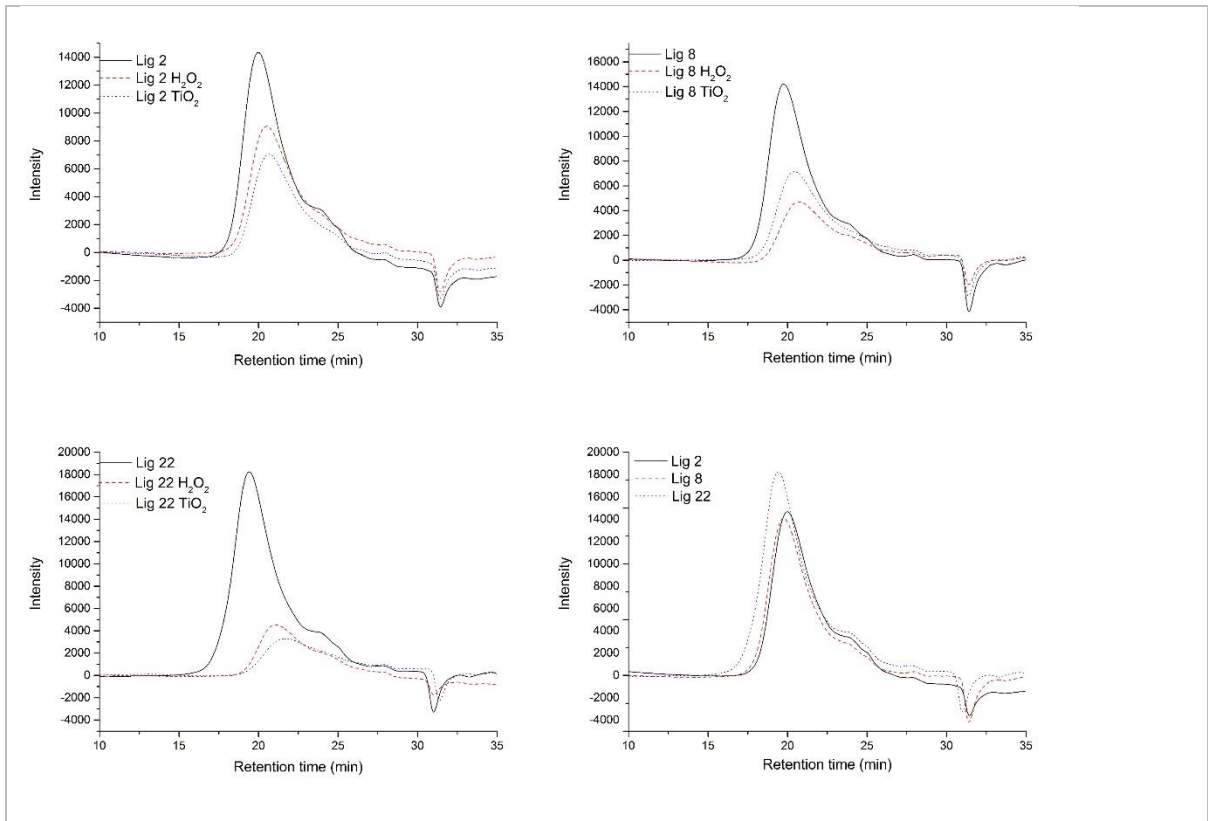


Figure 7: *MWD of different lignins*

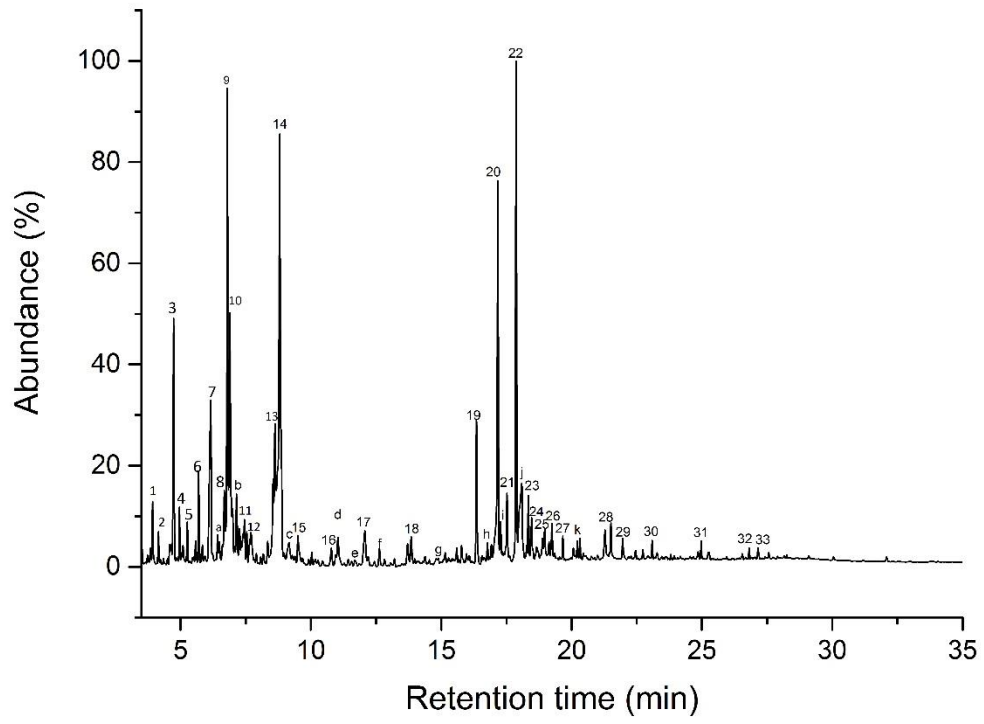


Figure 8: oil Chromatogram

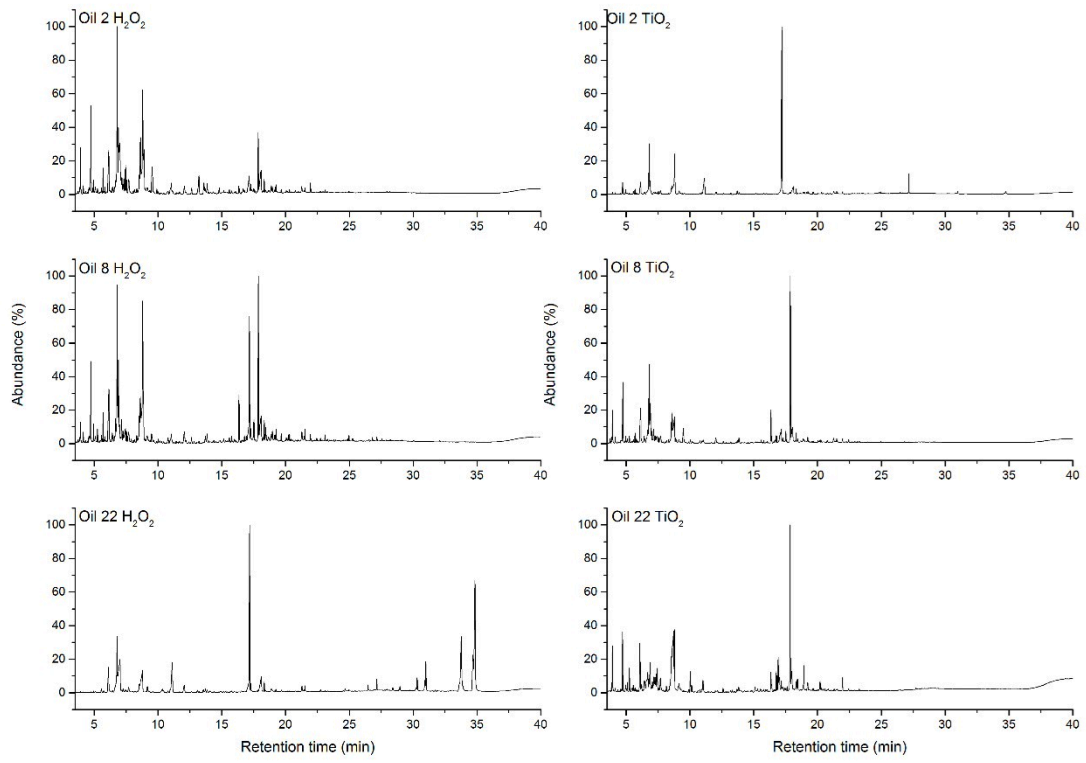


Figure 9: Oil chromatograms obtained by GCMS

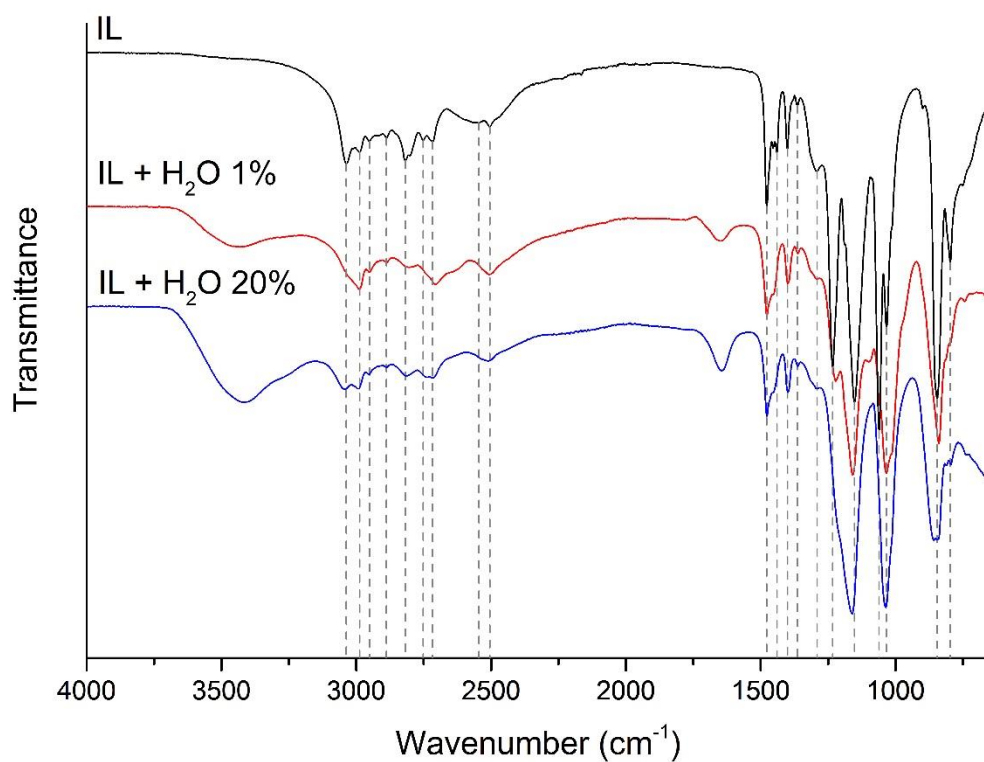
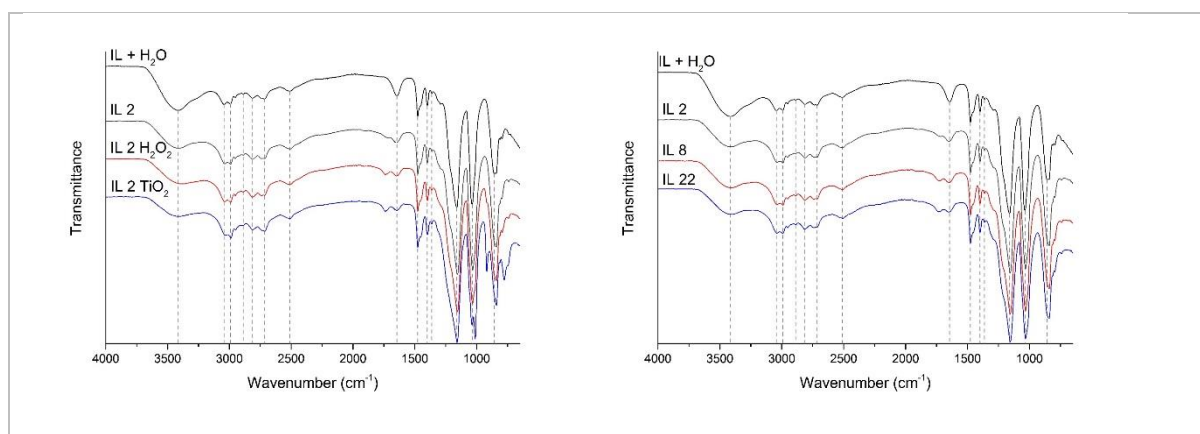


Figure 10: ATR-IR spectra of the IL and its mixture with water



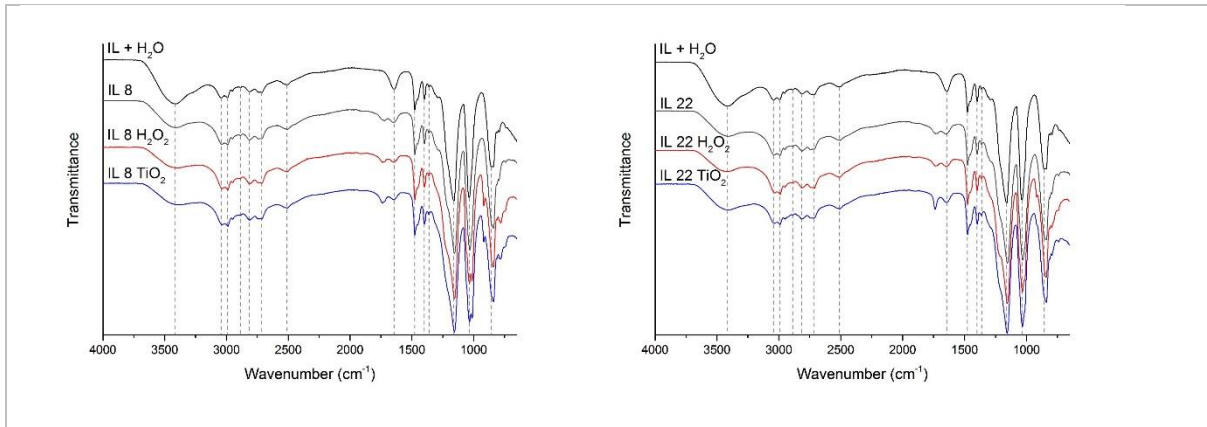
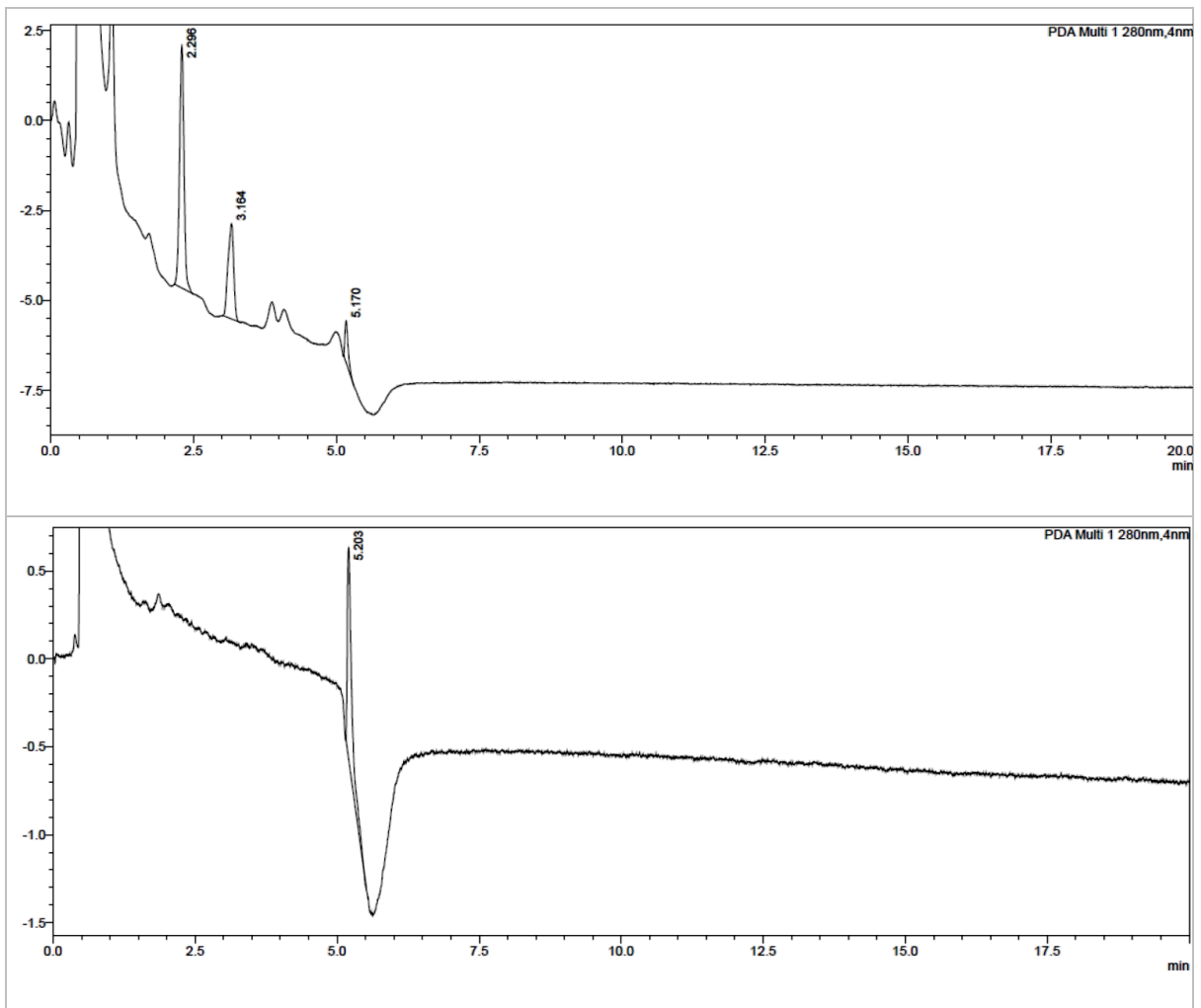
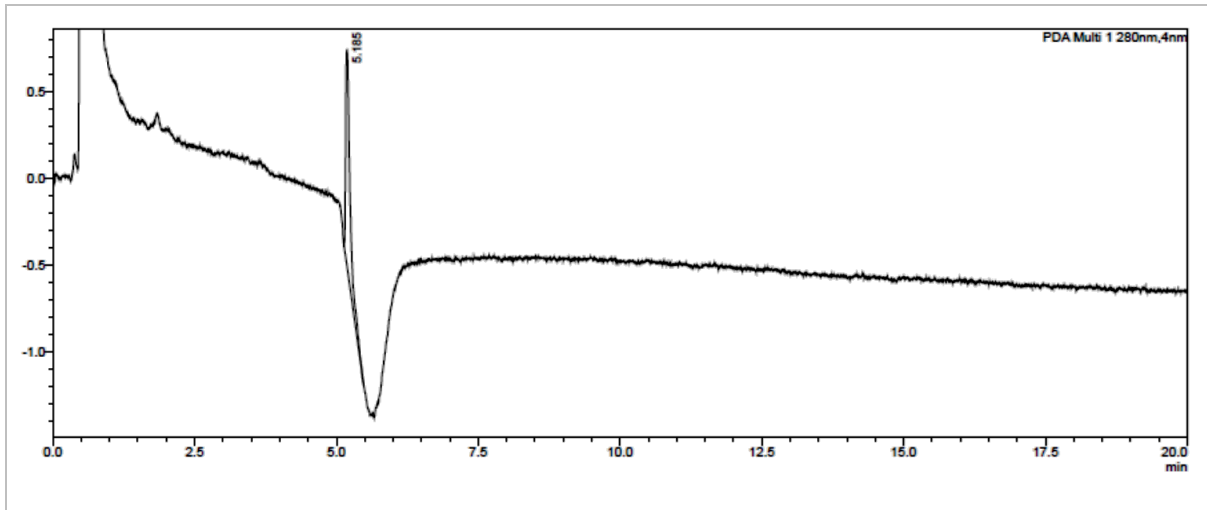


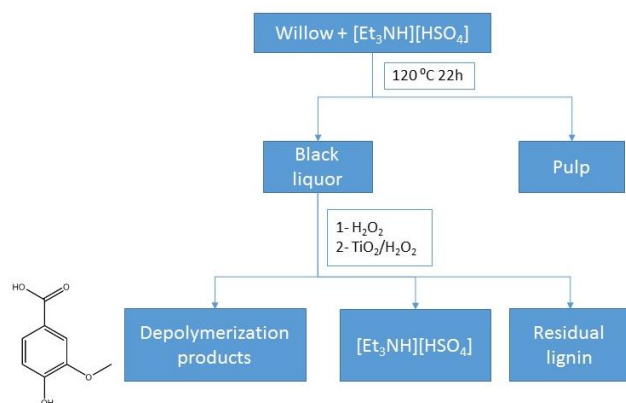
Figure 11: ATR-IR spectra of IL after the different treatments





*Figure 12: HPLC results for IL after the different conditions a) after pretreatment b) after treatment with H<sub>2</sub>O<sub>2</sub> c) after treatment with TiO<sub>2</sub>/H<sub>2</sub>O<sub>2</sub>*

## For Table of contents only



## Authors

Raquel Prado

Xabier Erdocia

Gilbert Francis De Gregorio

Jalel Labidi

Tom Welton

## Synopsis

Reusable ionic liquids are used as solvents and biomass as the feedstock to obtain chemicals from renewable resources.